

Quasiparticle dynamics and phonon softening in FeSe superconductors

C. W. Luo^{1*}, I. H. Wu¹, P. C. Cheng¹, J-Y Lin², K. H. Wu¹, T. M. Uen¹, J. Y. Juang¹, T. Kobayashi^{1,3}, D. A. Chareev⁴, O. S. Volkova⁵, and A. N. Vasiliev⁵

1. Department of Electrophysics, National Chiao Tung University, Hsinchu 300, Taiwan

2. Institute of Physics, National Chiao Tung University, Hsinchu 300, Taiwan

3. Department of Applied Physics and Chemistry and Institute for Laser Science, University of Electro-Communications, 1-5-1 Chofugaoka, Chofu, Tokyo 182-8585, Japan

4. Institute of Experimental Mineralogy, Chernogolovka, Moscow Region, 142432, Russia

5. Low Temperature Physics and Superconductivity Department, Moscow State University, 119991 Moscow, Russia

Quasiparticle dynamics of FeSe single crystals revealed by dual-color transient reflectivity measurements ($\Delta R/R$) provides unprecedented information on Fe-based superconductors. The amplitude of fast component in $\Delta R/R$ clearly tells a competing scenario between spin fluctuations and superconductivity. Together with the transport measurements, the relaxation time analysis further exhibits anomalous changes at 90 K and 230 K. The former manifests a structure phase transition as well as the associated phonon softening. The latter suggests a previously overlooked phase transition or crossover in FeSe. The electron-phonon coupling constant λ is found to be 0.16, identical to the value of theoretical calculations. Such a small λ demonstrates an unconventional origin of superconductivity in FeSe.

Since the discovery of Fe-based superconductors (FeSCs) in 2008 [1], tremendous experimental and theoretical efforts have been devoted to explore their characteristics. These Fe-based pnictide compounds exhibit a very interesting phase diagram, with antiferromagnetism (AFM) (or spin-density wave, SDW) at low doping and superconductivity at intermediate doping [2]. The simultaneous presence of magnetism and superconductivity in the phase diagram implies that magnetism plays an important role in the superconductivity mechanism. The existence of precursor superconductivity above T_c which competes with the SDW order [3], and a pseudogaplike feature with onset around 200 K [4] were observed on underdoped (Ba, K)Fe₂As₂ and nearly optimally doped SmFeAsO_{0.8}F_{0.2}, respectively. Additionally, a coherent lattice oscillation was also found in Co-doped BaFe₂As₂ using time-resolved pump-probe reflectivity with 40 fs time resolution [5]. Among various FeSCs, the iron chalcogenide FeSe [6] stands out due to its structure simplicity, which consists of iron-chalcogenide layers stacking one by another with the same Fe⁺² charge state as the iron pnictides. This so-called “11” system is so simple that it could be the key structure to understanding the origin of high- T_c superconductivity [7]. There has been considerable concern over the interplay between electronic structure, phonons, magnetism and superconductivity in 11-type FeSe. Therefore, further studies of their quasiparticle dynamics are indispensable to understanding the high- T_c mechanism in FeSCs. Here we report the first time-resolved femtosecond spectroscopy study of FeSe single crystals to elucidate the electronic structure and the quasiparticle (QP) dynamics.

In this study, FeSe single crystals were grown in evacuated quartz by the self-flux method with slow cooling [8]. The crystalline structure of the samples was examined by

x-ray diffraction. The femtosecond spectroscopy measurement was performed using a dual-color pump-probe system (for light source, the repetition rate: 5.2 MHz, the wavelength: 800 nm, the pulse duration: 100 fs) and an avalanche photodetector with the standard lock-in technique. The fluences of the pump beam and the probe beam are 2.48 and $0.35 \mu\text{J}/\text{cm}^2$, respectively. The pump pulses have corresponding photon energy (3.1 eV) where the higher absorption occurred in the absorption spectrum of FeSe [9] and hence can generate electronic excitations. The QP dynamics is studied by measuring the photoinduced transient reflectivity changes ($\Delta R/R$) of the probe beam with photon energy of 1.55 eV.

Electronic excitations generated by the pump pulses results in a swift rise of $\Delta R/R$ at zero time delay. The observed excitation is triggered by transferring the electrons from d valence band of Fe to d conduction band of Fe [10]. At zero time delay, number of the excited electrons generated by this non-thermal process is related to the amplitude of $\Delta R/R$. These high-energy electrons accumulated in the d conduction band of Fe release their energy through the emission of longitudinal-optical (LO) phonons within several picoseconds [11]. The LO phonons further decay into longitudinal-acoustic (LA) phonons via anharmonic interactions, i.e. transferring energy to the lattice. This relaxation process can be detected using a probe beam as shown in Fig. 1(a), which shows the 2D $\Delta R/R$ taken on an FeSe single crystal. There appear four temperature regions. Above 230 K, T^* (region I), there is a fast negative response with a relaxation time of about 1.5 ps together with a long period oscillation. When the temperature decreases into region II, a positive and slow response appears and $\Delta R/R$ gradually becomes smaller until $T=90$ K (T_S) where the resistivity $\rho(T)$ curve shows the kink (Fig. 1(b)). Below 90 K (region III), the slow positive

response disappears and is replaced by a complicated mixture of the positive and negative components as discussed later. For $T < T_c$ (region IV), a long-lived negative response appears as that one in region I. These four regions in 2D $\Delta R/R$ are apparently corresponding to the feature of $\rho(T)$ in FeSe. The relaxation processes ($t > 0$) of $\Delta R/R$ in FeSe can be phenomenologically described by

$$\frac{\Delta R}{R} = A_e e^{-\frac{t}{\tau_e}} + A_{LO} e^{-\frac{t}{\tau_{LO}}} + A_0 + A_{AL} e^{-\frac{t}{\tau_{AL}}} \sin\left(\frac{2\pi t}{T(t)} + \phi\right) \quad (1)$$

The first term in the right-hand side of Eq. (1) is the decay of the excited electrons with an initial population number, A_e , and a relaxation time, τ_e . The second term is the phonon number, A_{LO} , and a corresponding decay time, τ_{LO} . The third term describes energy loss from the hot spot to the ambient environment within the time scale of microsecond, which is far longer than the period of the measurement (~ 150 ps) and hence is taken as a constant. The last term is the chirped oscillation component associated with strain pulse propagation: A_{LA} is the amplitude of the oscillation; τ_{LA} is the damping time; $T(t)$ is the time-dependent period; ϕ is the initial phase of the oscillation.

We first discuss the temperature-dependent $\Delta R/R$ in FeSe. Fig. 1(a) shows $\Delta R/R$ from 290 K down to 4.4 K, from which each component described above can be extracted using Eq. (1). Results of the extraction are shown in Fig. 2(a), (b), (c) and (d). For the fast component in $\Delta R/R$, A remarkable increase in the amplitude (A_e) is shown in Fig. 2(a) when T decreases from 90 K. This trend is closely related to the strong antiferromagnetic spin fluctuations below $T=T_S$ as revealed by ^{77}Se NMR measurements [12]. Intriguingly as $T < T_c$ (region IV in Fig. 1), A_e decreases due to the onset of superconductivity. This suggests that the spin fluctuations and superconductivity be competing factors in the FeSe system.

The above results provide the first compelling experimental evidence of competing orders in FeSe, which are consistent with the theoretical calculations [13]. It is noted that the experimental evidence on the competing orders was also reported in underdoped (Ba, K)Fe₂As₂ [3]. According to Rothwarf-Taylor (RT) model [14], the density of thermally excited QPs $n_T \propto [A_1(T)/A_1(T \rightarrow 0)] - 1$ as shown in the inset of Fig. 2(a). The temperature-dependent behavior of n_T can be further fitted by $n_T \propto [\Delta(T)T]^{1/2} \exp(-\Delta(T)/T)$ where $\Delta(T)$ is the superconducting energy gap. Assuming a BCS temperature dependent $\Delta(T) = \Delta(0)[1 - (T/T_c)]^{1/2}$, the fits lead to $\Delta(0) = 3.24 k_B T_c$, in accord to the value obtained from specific heat measurements [15]. (This isotropic $\Delta(T)$ scenario is certainly too simplified, but it suffices to estimate the scale of $\Delta(T)$.) The presence of a gap in the QP density of states (DOS) gives rise to a bottleneck for carrier relaxation, which is clearly observed in the relaxation time τ_e close to T_c . For the slower component, the amplitude A_{LO} monochromatically decreases as T does; then it completely disappears in the superconducting state. On the contrary, the relaxation time τ_{LO} exhibits two marked anomalies both at $T^* \sim 230$ K and $T_S \sim 90$ K, corresponding to the boundary between region I and II, and that between region II and III, respectively. During the structural transition from a tetragonal phase to an orthorhombic phase [16], the energy of photoinduced QPs efficiently releases to lattice through LO phonons and resulted in a significant short relaxation time τ_{LO} . On the other hand, the abnormal long relaxation time τ_{LO} around 230 K suggests an elusive higher-temperature phase transition or crossover to undermine the energy release efficiency. The sign change of Seebeck coefficient of FeSe was found to be also at T^* [17].

By fitting the $\Delta R/R$ curves with Eq. (1), dynamic information of QPs and phonons is

available, which includes, the number of QPs, the relaxation time of QPs, and the energy of phonons. In a metal, the photoinduced QPs relaxation time is governed by transferring energy from electron to phonon with electron-phonon coupling strength λ [18].

$$\frac{1}{\tau_e} = \frac{3\hbar\lambda\langle\omega^2\rangle}{\pi k_B T_e} \quad (2)$$

Where $\lambda\langle\omega^2\rangle$ is the second moment of the Eliashberg function and T_e can be further described by [19]

$$T_e = \left\langle \sqrt{T_i^2 + \frac{2(1-R)F}{l_s\gamma} e^{-z/l_s}} \right\rangle \quad (3)$$

where R is the unperturbed reflectivity at 400 nm, F is the pumping fluences and γ is the linear coefficient of heat capacity due to the electronic subsystem. The mean value is taken for the depth z going from the crystal surface down to the skin depth $l_s \sim 64$ nm (it was estimated from the skin depth of EM wave in metal, $\lambda/2\pi$). All of the parameters for the calculations of electron-phonon coupling strength were listed in Table I. For the estimate of $\langle\omega^2\rangle$, some vibrational modes are more efficiently coupled to QP's than others is. In the case of Co-doped BaFe₂As₂, the symmetric A_{1g} mode is coherently excited by photoexcitation and efficiently coupled [5]. Consequently, we take the A_{1g} mode into account in the present case of FeSe, which is the strongest phonon mode in electron-phonon spectral function, $\alpha^2F(\omega)$ [10]. By Eq. (2), the consequent electron-phonon (A_{1g} mode) coupling constant, $\lambda=0.16$ in FeSe. This value is consistent with the theoretical results of $\lambda=0.17$ [10] obtained by using linear response within the generalized gradient approximation (GGA). Furthermore, we can use the McMillan formula $T_c = (\langle\omega\rangle/1.2)\exp\{-[1.40(1+\lambda)]/[\lambda-\mu^*(1+0.62\lambda)]\}$ to evaluate the critical

temperature T_c [21]. Taking $\langle\hbar\omega\rangle= 19.9$ meV and $\mu^*=0$, we obtain $T_c \sim 0.08$ K, which is one order of magnitude lower than the actual T_c of about 9 K. Actually, the *total* coupling strength between quasiparticles and bosons is estimated to be 1.55 from the specific heat measurements [15]. Therefore, the present study experimentally verifies that the superconductivity in FeSe should be attributed to the unconventional mechanism other than electron-phonon coupling.

Further insight into the phase transition in FeSe is provided by the study of the oscillation component of $\Delta R/R$. Temperature dependence of a strain pulse (longitudinal-acoustic (LA) phonons) propagation was clearly observed in the oscillation feature of $\Delta R/R$ after subtracting the decay background (i.e. the 1st, 2nd and 3rd terms in Eq. (1)), as shown in the inset of Fig. 3. This oscillation is caused by the propagation of strain pulses inside FeSe single crystals, namely the interference between the probe beams reflected by the crystal surface and the wave front of the propagating strain pulse [22]. In order to quantify the properties of LA phonons in FeSe, the locations of the peaks and deeps of the oscillation in the inset of Fig. 3 is shown as the function of temperatures in Fig. 3. At high temperatures, the damping time is very short and the oscillation sustains only for one period. However, the number of oscillation period significantly increases below 100 K; hence the damping time becomes much longer. This means that the LA phonons can propagate further into the interior of FeSe crystals with the orthorhombic structure. According to the difference between 1st deep (at 23.52 ps) and 2nd deep (at 72.78 ps) at $T = 110$ K, the phonon frequency is found to be 20.3 GHz. The phonon energy is estimated to be ~ 0.087 meV. The coherent acoustic phonon detected by a pump-probe reflectivity measurement can be described as a Brillouin scattering [23] phenomenon occurring in the

materials after the excitation of pump pulses. The scattering condition is

$$q_{\text{phonon}} = 2nk_{\text{probe}} \cos(\theta_i) \quad (4)$$

where q_{phonon} is the phonon wave vector, n is the real part of the refractive index, and the probe photon has a wave vector k_{probe} arriving at an incident angle θ_i (inside crystals) with respect to the surface normal. Following this scattering condition, the probe beam acts as a filter to select the acoustic wave propagating along the scattering plane symmetry axis, i.e. the normal to the crystal surface and traveling with the wave vector q_{phonon} . The energy of the acoustic wave is

$$E_{\text{phonon}} = \hbar f_{\text{phonon}} = \hbar q_{\text{phonon}} v_s = \hbar 2n v_s k_{\text{probe}} \cos(\theta_i) \quad (5)$$

where v_s is the sound velocity along normal direction of crystal surface. Using $\lambda_{\text{probe}} = 800$ nm, $n_{\text{probe}} = 2$ [9], $\theta_i = 2.5^\circ$ (estimated from the incident angle (5°) of the probe beam by Snell's law) and $v_s = 3.58$ km/s [24], the phonon energy, E_{phonon} , is calculated to be 0.077 meV, which is very close to the result, 0.087 meV, directly obtained from the above $\Delta R/R$ measurements.

We further investigate the temperature dependence of the LA phonon energy as shown in Fig. 4. The phonon energy dramatically drops by 60% around 90 K where a structural phase transition occurs, and then keeps constant at low temperatures. Additionally, we found that the LA phonons also soften by 6% in the superconducting state as shown in the inset of Fig. 4, which is consistent with the larger distance between 1st deep and 1st peak in Fig. 3. Very recently, this softening of lattice has been found in Co-doped BaFe₂As₂ by resonant ultrasound spectroscopy [25, 26]. Fernandes *et al.* [25] found the 16% softening of shear modulus in BaFe_{1.84}Co_{0.16}As₂ at $T_c = 22$ K. For the non-superconducting case of BaFe₂As₂, however, the rather large softening of 90% was

observed around 130 K where is the structural and AFM phase transition temperature. Similarly, a large phonon softening due to structural phase transition and a rather small phonon softening due to the superconductive phase transition was also observed in 11-type FeSe in this Letter. These results suggest that the reduction of phonon energy at both the structural and the superconducting phase transition is a general feature in FeSCs. The above phonon softening may participate in the superconducting pairing, albeit not the mechanism responsible for high T_c in FeSCs.

In summary, we have studied the ultrafast quasiparticle dynamics and phonon softening in FeSe single crystals by dual-color femtosecond spectroscopy. The temperature dependence of the amplitude A_e suggests a competing scenario between spin fluctuations and the superconductivity. The relaxation time τ_e of $\Delta R/R$ reveals a electron-phonon coupling constant $\lambda=0.16$. The structure phase transition at 90 K is elucidated through both the electrical transport properties and the anomalous changes of relaxation time τ_{LO} of $\Delta R/R$. A previously unknown feature at 230 K is further identified. Moreover, the energy of LA phonons at 110 K was estimated to be 0.087 meV from the oscillation component of $\Delta R/R$, which markedly softens around both the structural phase transition and superconducting transition. Our results provide the vital understanding of the competing picture between the spin fluctuations and superconductivity, and of the role of phonons in Fe-based superconductors.

Acknowledgements

This project is financially sponsored by National Science Council (Grants No. NSC 98-2112-M-009-008-MY3) and the Ministry of Education (MOE-ATU plan at National

Chiao Tung University). We would like to thank Y. S. Hsieh for technical support.

References

- [1] Y. Kamihara, T. Watanabe, M. Hirano, and H. Hosono, *J. Am. Chem. Soc.* **130**, 3296 (2008).
- [2] Johnpierre Paglione and Richard L. Greene, *Nature Phys.* **6**, 645 (2010).
- [3] E. E. M. Chia *et al.*, *Phys. Rev. Lett.* **104**, 027003 (2010).
- [4] T. Mertelj *et al.*, *Phys. Rev. Lett.* **102**, 117002 (2009).
- [5] B. Mansart *et al.*, *Phys. Rev. B* **80**, 172504 (2009).
- [6] F. C. Hsu *et al.*, *PNAS* **105**, 14262 (2008).
- [7] D. C. Johnston, *Advances in Phys.* **59**, 803 (2010).
- [8] V. Tsurkan *et al.*, arXiv : 1006.4453 v1 (2010).
- [9] X. J. Wu *et al.*, *Appl. Phys. Lett.* **90**, 112105 (2007).
- [10] A. Subedi *et al.*, *Phys. Rev. B* **78**, 134514 (2008).
- [11] F. S. Krasniqi *et al.*, *Phys. Rev. B* **78**, 174302 (2008).
- [12] T. Imai *et al.*, *Phys. Rev. Lett.* **102**, 177005 (2009).
- [13] Hongliang Shi *et al.*, *J. Appl. Phys.* **110**, 043917 (2011).
- [14] A. Rothwarf and B. N. Taylor, *Phys. Rev. Lett.* **19**, 27 (1967).
- [15] J.-Y. Lin *et al.*, arXiv. 1109.5225.
- [16] T. M. McQueen *et al.*, *Phys. Rev. Lett.* **103**, 057002 (2009).
- [17] T. M. McQueen *et al.*, *Phys. Rev. B* **79**, 014522 (2009).
- [18] P. B. Allen, *Phys. Rev. Lett.* **59**, 1460 (1987).
- [19] D. Boschetto *et al.*, *Phys. Rev. Lett.* **100**, 027404 (2008).
- [20] P. Kumar *et al.*, *Solid State Commun.* **150**, 557 (2010).
- [21] W. L. McMillan, *Phys. Rev.* **167**, 331 (1968).

- [22] C. Thomsen, H. T. Grahn, H. J. Maris, and J. Tauc, *Phys. Rev. B* **34**, 4129 (1986).
- [23] L. Brillouin, *Ann. Phys. (Paris)* **17**, 88 (1922)
- [24] S. Chandra and A. K. M. A. Islam, *Physica C* **470**, 2072 (2010).
- [25] R. M. Fernandes *et al.*, *Phys. Rev. Lett.* **105**, 157003 (2010).
- [26] T. Goto *et al.*, *J. Phys. Soc. Jpn.* **80**, 073702 (2011).

TABLE CAPTIONS

TABLE I. The parameters for λ estimating at $T=20$ K of a FeSe single crystal.

Figure captions

Fig. 1 (color online) (a) Temperature and delay time dependence of $\Delta R/R$ in a FeSe single crystal. The inset shows a part of the $\Delta R/R$ on an enlarged scale. Solid lines indicate $\Delta R/R = 0$. (b) Temperature dependence of the resistivity ρ indicates the high quality of a FeSe single crystal. The kink of $\rho(T)$ at 90 K manifests the structure phase transition.

Fig. 2 (color online) Temperature dependence of the amplitude (a) A_e , (c) A_{LO} and the relaxation time (b) τ_e , (d) τ_{LO} by fitting Eq. (1). Inset of (a): Density of thermally-excited QPs, $n_T(T)$. Solid line fits to the PT model. Inset of (b) shows a part of temperature-dependent τ_e on an enlarged scale. Dashed lines are guides to the eyes.

Fig. 3 (color online) Temperature-dependent peaks and deeps of the oscillation component in $\Delta R/R$. Inset: temperature and delay time dependence of the 3D oscillation component was obtained by subtracted the decay background (the 1st, 2nd and 3rd terms in Eq. (1)) from $\Delta R/R$ of Fig. 1(a). Solid lines are a guide to the eyes.

Fig. 4 (color online) Temperature dependence of the phonon energy derived from the oscillation component in Fig. 3. Inset shows a part of the temperature-dependent phonon energy on an enlarged scale. Solid lines are a guide to the eyes.

	T_c (K)	R (400 nm)	F ($\mu\text{J}/\text{cm}^2$)	γ^a ($\text{mJ mol}^{-1}\text{K}^{-1}$)	T_e^b (K)	τ_1 (ps)	A_{1g}^c (meV)	$\lambda\langle\omega^2\rangle^d$ (meV^2)	λ
FeSe	9	0.15	2.48	5.73	45.8	1.75	19.9	61.3	0.16

^a From Ref. [15].

^b Obtained From Eq. (3).

^c From Ref. [20].

^d Obtained Eq. (2).

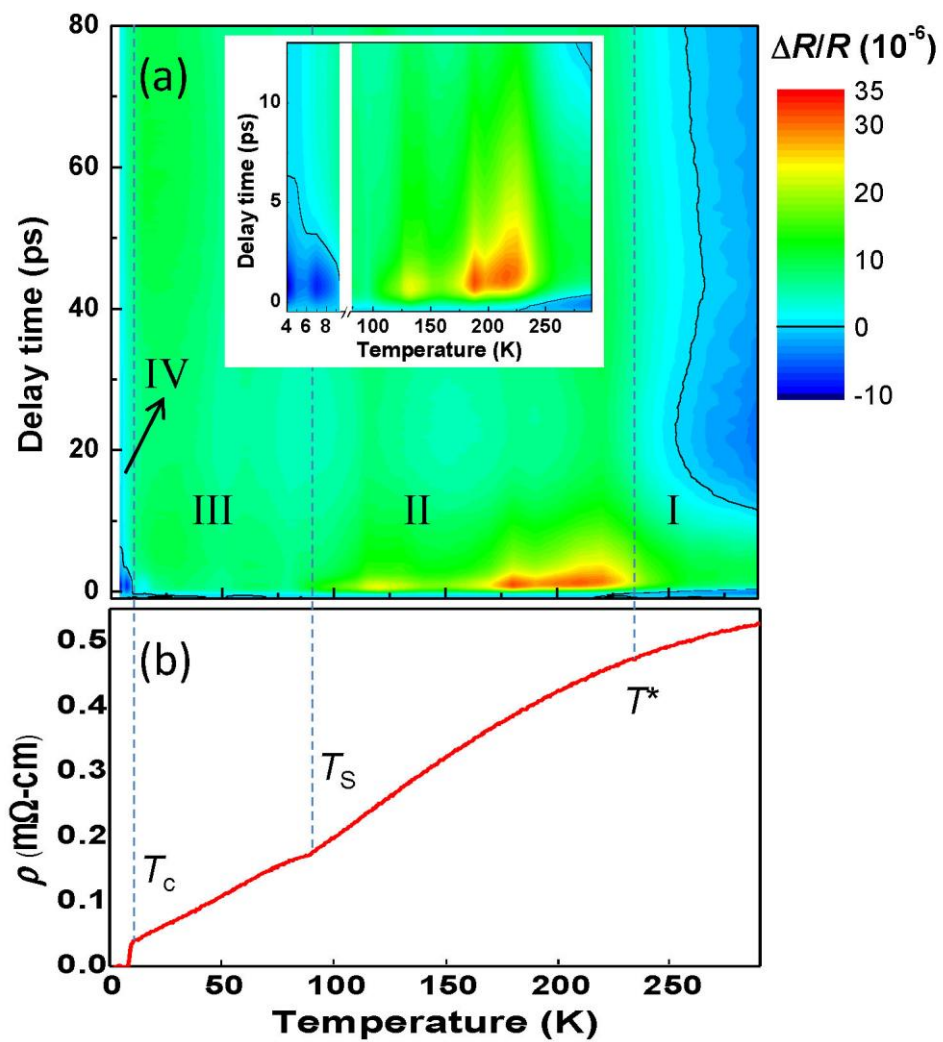


Fig 1

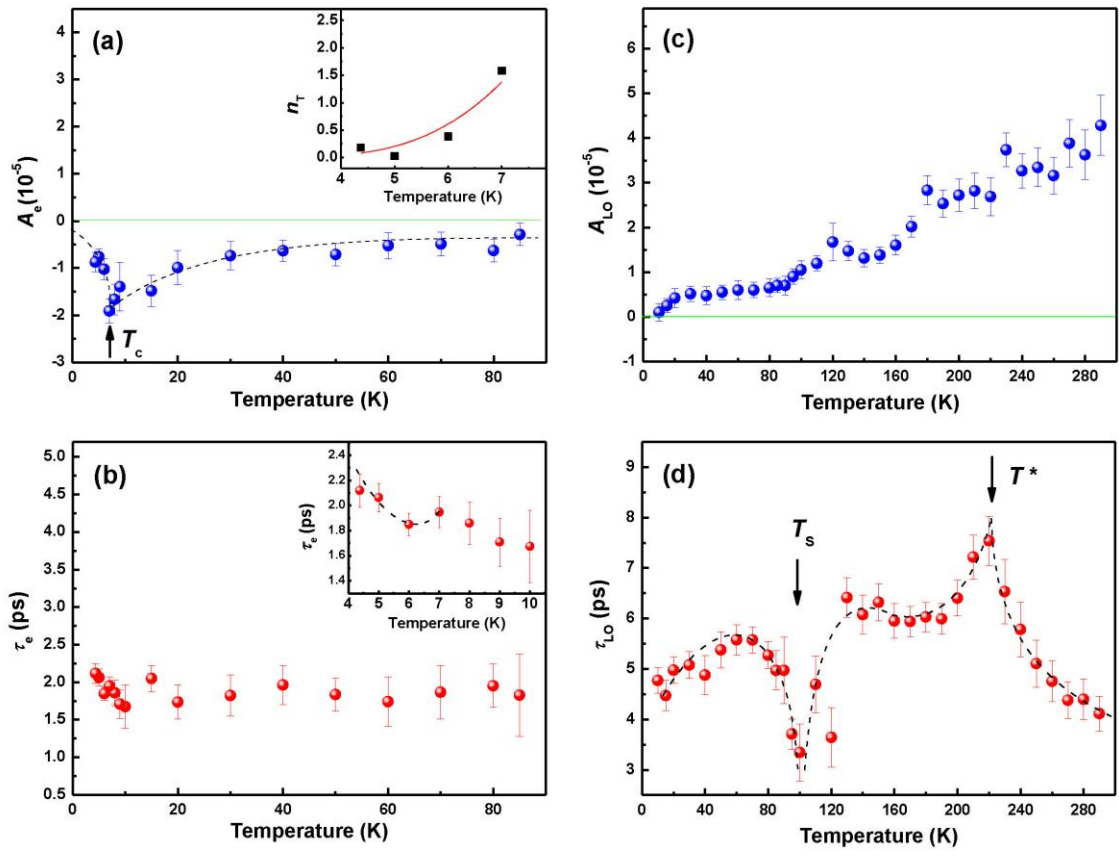


Fig 2

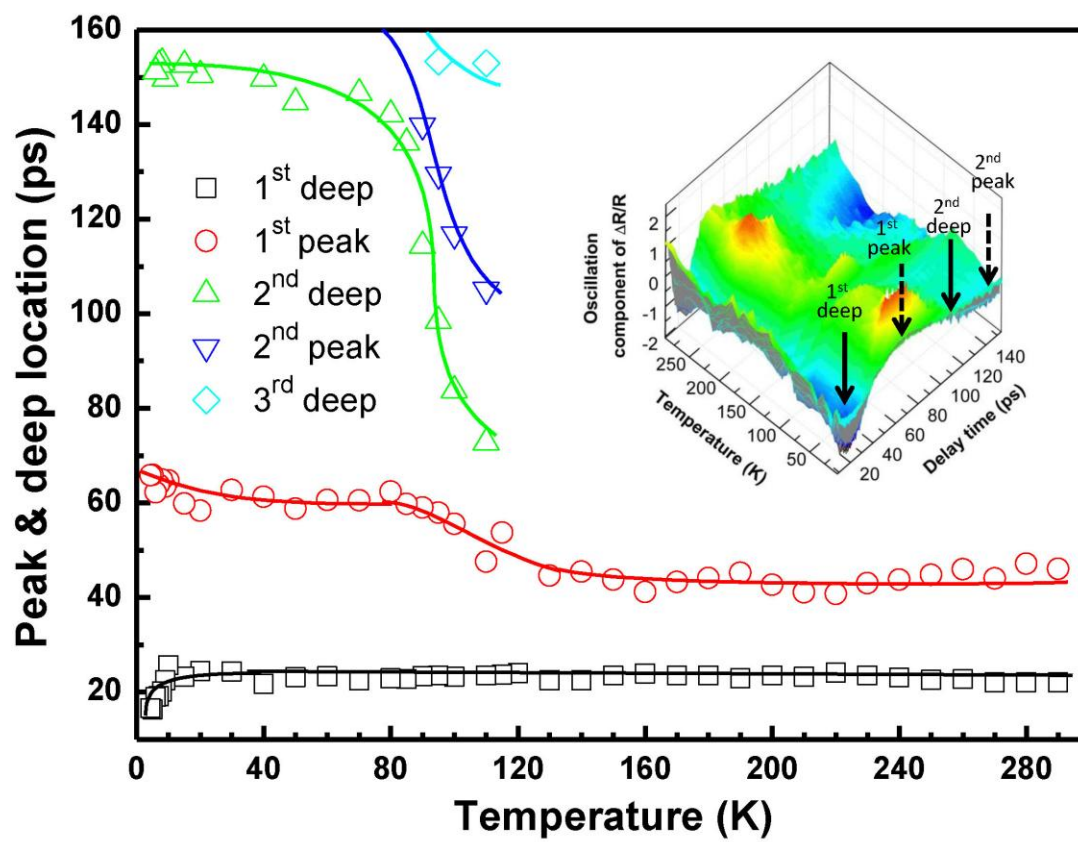


Fig 3

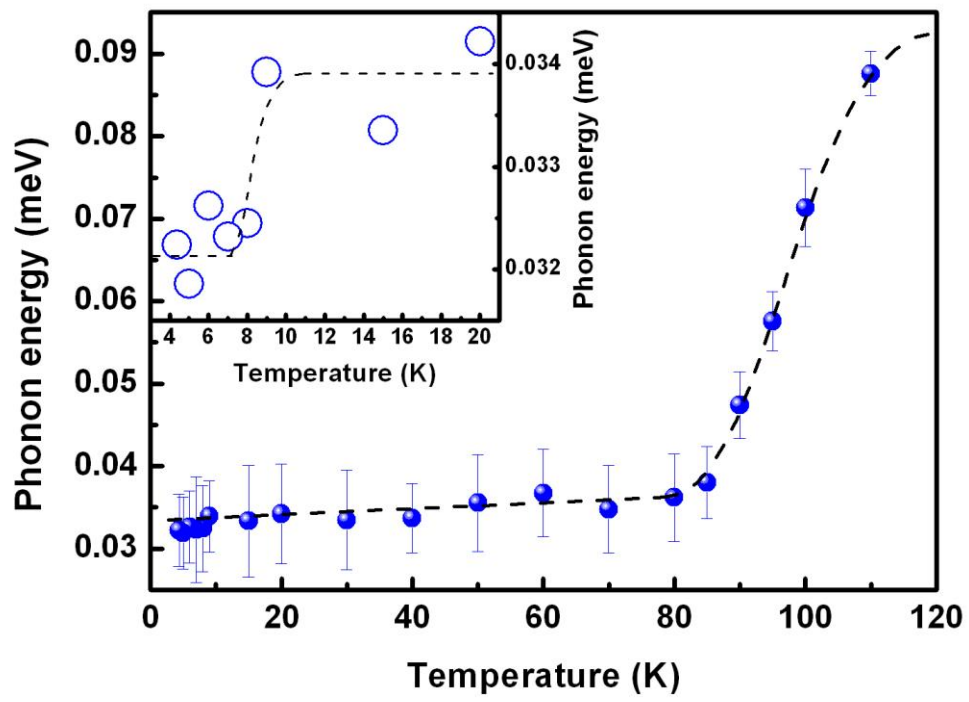


Fig 4